



1 Routine monitoring of Western Lake Erie to track water quality  
2 changes associated with cyanobacterial harmful algal blooms

3  
4 Anna G. Boegehold<sup>1</sup>, Ashley M. Burtner<sup>1</sup>, Andrew C. Camilleri<sup>1</sup>, Glenn Carter<sup>1</sup>, Paul DenUyl<sup>1</sup>,  
5 David Fanslow<sup>2</sup>, Deanna Fyffe Semenyuk<sup>1,3</sup>, Casey M. Godwin<sup>1</sup>, Duane Gossiaux<sup>2</sup>, Thomas H.  
6 Johengen<sup>1</sup>, Holly Kelchner<sup>1</sup>, Christine Kitchens<sup>1</sup>, Lacey A. Mason<sup>2</sup>, Kelly McCabe<sup>1</sup>, Danna  
7 Palladino<sup>2</sup>, Dack Stuart<sup>1,4</sup>, Henry Vanderploeg<sup>2</sup>, Reagan Errera<sup>2</sup>

8  
9  
10 <sup>1</sup>Cooperative Institute for Great Lakes Research (CIGLR), University of Michigan, 4840 South  
11 State Road, Ann Arbor, MI 48108, USA

12 <sup>2</sup>NOAA Great Lakes Environmental Research Laboratory, 4840 South State Road, Ann Arbor,  
13 MI 48108, USA

14 <sup>3</sup>Jacobs, 1999 Bryan Street, Suite 1200, Dallas, TX, 75201, USA

15 <sup>4</sup>Woods Hole Group, Inc., 107 Waterhouse Road, Bourne, MA 02532

16  
17 *Correspondence to:* Anna G Boegehold ([annaboeg@umich.edu](mailto:annaboeg@umich.edu)) & Reagan Errera  
18 ([reagan.errera@noaa.gov](mailto:reagan.errera@noaa.gov))



## 19 Abstract

20 The western basin of Lake Erie has a history of recurrent cyanobacterial harmful algal blooms  
21 (HABs) despite decades of efforts by the United States and Canada to limit nutrient loading, a  
22 major driver of the blooms. In response, the National Oceanic and Atmospheric Administration  
23 (NOAA) Great Lakes Environmental Research Laboratory (GLERL) and the Cooperative  
24 Institute for Great Lakes Research (CIGLR) created an annual sampling program to detect,  
25 monitor, assess, and predict HABs in western Lake Erie. Here we describe the data collected  
26 from this monitoring program from 2012 to 2021. This dataset includes observations on physico-  
27 chemical properties, major nutrient fractions, phytoplankton pigments, microcystins, and optical  
28 properties for western Lake Erie. This dataset is particularly relevant for creating models,  
29 verifying and calibrating remote sensing algorithms, and informing experimental research to  
30 further understand the water quality dynamics that enable HABs in this internationally significant  
31 body of freshwater. The dataset can be freely accessed from NOAA National Centers for  
32 Environmental Information (NCEI) at <https://doi.org/10.25921/11da-3x54> (Cooperative  
33 Institute for Great Lakes Research, University of Michigan; NOAA Great Lakes Environmental  
34 Research Laboratory, 2019).



## 35 Introduction

36 Lake Erie is situated on the international boundary between the United States and  
37 Canada and is the smallest by volume of the five Laurentian Great Lakes. It is ecologically,  
38 culturally, and economically significant to the approximately 12.5 million people who live in the  
39 watershed. Each year Lake Erie supports nearly 14,000 tonnes of commercial and traditional  
40 fisheries, over 33,000,000 tonnes of freight, and over \$1.5 million in recreation and tourism  
41 business (Sternier et al., 2020). Lake Erie has endured multiple anthropogenic stressors since  
42 European settlement in the area, most notably the draining of coastal wetlands for development  
43 of agricultural lands in the late 18th century (Allinger and Reavie, 2013). Currently, the  
44 ecological state of Lake Erie is considered poor, partially due to excess nutrient input that  
45 supports harmful algal blooms (HABs; ECCO and US EPA, 2022). These seasonal HABs are  
46 typically dominated by toxin producing cyanobacteria, causing concern for public and  
47 ecosystem health (Watson et al., 2016). Humans can be exposed to cyanotoxins through  
48 ingestion of contaminated fish and drinking water and through inhalation and dermal exposure  
49 during recreational events such as swimming and boating (Carmichael and Boyer, 2016; Buratti  
50 et al., 2017). Cyanotoxins can also cause illness and death in aquatic and terrestrial animals  
51 (Carmichael and Boyer, 2016). The economic cost of HABs impacts in Lake Erie is estimated to  
52 be hundreds of millions of dollars each year (Smith et al., 2019).

53 To combat the deteriorated state of Lake Erie water quality, bi-national water resource  
54 management policies alongside scientific research and water quality monitoring efforts have  
55 been underway for decades. The Great Lakes Water Quality Agreement (GLWQA), first signed  
56 in 1972, was a commitment between the US and Canada in response to degraded water quality  
57 throughout the Great Lakes ecosystem (GLWQA, 2012). Phosphorus was found to be the key  
58 nutrient that was promoting excess phytoplankton growth (Charlton et al., 1993), and thus the  
59 GLWQA sought to limit total phosphorus input to the lakes in an attempt to reduce



60 phytoplankton growth and biomass (Steffen et al., 2014). The 1972 Clean Water Act (CWA) was  
61 similarly enacted to regulate pollution discharge, including phosphorus, into navigable waters in  
62 the United States. After the signing and implementation of the phosphorus load reduction  
63 practices outlined in the GLWQA and CWA, the water quality of Lake Erie improved and the  
64 lake experienced a period of restoration (Makarewicz and Bertram, 1991). This success was  
65 attributed to upgrades to sewage treatment plants and industrial discharges which reduced  
66 phosphorus loading from point sources by 50% within ten years of peak levels observed in 1968  
67 (Charlton et al., 1993; Joosse and Baker, 2011; Steffen et al., 2014).

68 While the water quality of Lake Erie rebounded in the 1980s and early 1990s, by the mid  
69 1990s and early 2000s annual HAB events were occurring in Lake Erie again, particularly in the  
70 warm, shallow western basin (Allinger and Reavie, 2013; Kane et al., 2015; Watson et al.,  
71 2016). Total phosphorus loading has been relatively stable in Lake Erie from the 1980s onward  
72 (Dolan and Chapra, 2012; Watson et al., 2016), and although phosphorus loading controls had  
73 been a successful mitigation measure at one point, several anthropogenic stressors within the  
74 watershed were exacerbating the issue of poor water quality. An increase in agricultural sources  
75 of biologically available soluble nutrients, legacy phosphorus in the Lake Erie watershed, altered  
76 nutrient cycling by invasive dreissenid mussels, and climate change are thought to be primarily  
77 responsible for the HABs resurgence (Vanderploeg et al., 2001; Conroy et al., 2005; Bridoux et  
78 al., 2010; Michalak et al., 2013; Matisoff et al., 2016; Huisman et al., 2018; Van Meter et al.,  
79 2021).

80 The post-recovery period HABs have predominantly been composed of the  
81 cyanobacteria species *Microcystis aeruginosa* along with genera *Anabaena*, *Aphanizomenon*,  
82 *Dolichospermum*, and *Planktothrix* (Steffen et al., 2014; Watson et al., 2016). These  
83 cyanobacteria can produce an array of several types of phycotoxins, with the most common  
84 being a suite of hepatotoxins known as microcystins (MCs). Microcystins primarily affect the  
85 liver but can also cause adverse health effects on the kidneys, brain, and reproductive organs



86 (Carmichael and Boyer, 2016). Phycotoxins are commonly present during Lake Erie HABs, and  
87 in August 2014 the city of Toledo, OH drinking water supply was contaminated with MCs,  
88 leaving >400,000 without clean drinking water (Steffen et al., 2017).

89 To understand HAB events in US waterways, Congress authorized the Harmful Algal  
90 Bloom and Hypoxia Research and Control Act in 1998 (HABHRCA; Public Law 115-423) which  
91 mandated the National Oceanic and Atmospheric Administration (NOAA) to “advance the  
92 scientific understanding and ability to detect, monitor, assess, and predict HAB and hypoxia  
93 events”. Under HABHRCA, the NOAA Great Lakes Environmental Research Lab (GLERL),  
94 NOAA National Centers for Coastal Ocean Science (NCCOS), and the Cooperative Institute for  
95 Great Lakes Research (CIGLR; formerly CILER - Cooperative Institute for Limnology and  
96 Ecosystems Research) developed an ecological forecast to predict HAB events in Lake Erie.  
97 Starting in 2008, researchers at these institutes began using remote sensing to monitor  
98 seasonal HABs, created a seasonal forecast system based on spring P loads, and developed  
99 models to predict short-term bloom changes to alert stakeholders and the public (Rowe et al.,  
100 2016). Products from these efforts, known as Lake Erie Harmful Algal Bloom Forecasts, are  
101 freely available during the bloom season at [https://coastalscience.noaa.gov/research/stressor-](https://coastalscience.noaa.gov/research/stressor-impacts-mitigation/hab-forecasts/lake-erie/)  
102 [impacts-mitigation/hab-forecasts/lake-erie/](https://coastalscience.noaa.gov/research/stressor-impacts-mitigation/hab-forecasts/lake-erie/).

103 *In-situ* sampling of the bloom was necessary to calibrate and validate the remote  
104 sensing images and models as well as measure microcystin concentration. Sampling events  
105 were led by personnel at GLERL and CIGLR starting in 2008 and were designed to collect  
106 discrete samples within the extent of the bloom area. At first, samples were taken  
107 opportunistically within the bloom and sampling locations and analytical parameters were  
108 inconsistent. In 2009, regular sampling stations were identified based on spatial patterns of the  
109 bloom. From 2009 to 2011, in addition to opportunistic samples, nine main stations in the  
110 western basin of Lake Erie were sampled intermittently from June through October (Bertani et  
111 al., 2017; Rowland et al., 2020). While these sampling efforts initially began to complement



112 existing research products, the experimental nature of the 2008 to 2011 sampling cruises also  
113 provided insight into creating a regular monitoring program that would support critical research  
114 and product development related to western Lake Erie HABs.

115 In 2012, researchers at GLERL and CIGLR, with support from the Great Lakes  
116 Restoration Initiative (GLRI), formalized a sampling regimen to monitor the spatial and temporal  
117 variability of seasonal HAB events in western Lake Erie (WLE). The establishment of this  
118 monitoring program corresponded with increased federal emphasis on evaluating trends and  
119 drivers of WLE HABs and water quality. Four monitoring stations were identified and regular  
120 surface samples were collected from May to September and analyzed for nutrient, pigment, and  
121 particulate microcystin concentrations (Figs. 1 & 2). In following years, the monitoring program  
122 evolved and expanded. New stations were added to better characterize the bloom and  
123 complement other observing systems. Sampling parameters were adjusted and added based on  
124 the needs of current research (Table 1). Results of these sampling cruises were compiled and  
125 distributed informally upon request until 2019 when the data were organized and archived on  
126 the NOAA National Centers for Environmental Information (NCEI) open-access data repository  
127 (<https://www.ncei.noaa.gov/>).

128 Long term monitoring of WLE is fundamental to the continual assessment of water  
129 quality changes in response to both stressors and water quality management efforts (Hartig et  
130 al., 2009, 2021). The GLERL/CIGLR monitoring data has been used by numerous researchers  
131 to develop and assess models (Rowe et al., 2016; Weiskerger et al., 2018; Fang et al., 2019;  
132 Liu et al., 2020; Qian et al., 2021; Wang and Boegman, 2021; Hellweger et al., 2022; Maguire et  
133 al., 2022), to calibrate remote sensing algorithms (Sayers et al., 2016, 2019; Avouris and Ortiz,  
134 2019; Bosse et al., 2019; Vander Woude et al., 2019; Pirasteh et al., 2020; Xu et al., 2022), and  
135 to elucidate ecological mechanisms and complement experimental data (Cory et al., 2016;  
136 Reavie et al., 2016; Berry et al., 2017; Steffen et al., 2017; Kharbush et al., 2019, 2023; Newell



137 et al., 2019; Den Uyl et al., 2021; Smith et al., 2021, 2022; Hoffman et al., 2022; Marino et al.,  
138 2022; Yancey et al., 2022a, b).

139 The objective of this paper is to inform users of the dataset “Physical, chemical, and  
140 biological water quality monitoring data to support detection of Harmful Algal Blooms (HABs) in  
141 western Lake Erie, collected by the Great Lakes Environmental Research Laboratory and the  
142 Cooperative Institute for Great Lakes Research since 2012” by describing the data generated  
143 from this monitoring program and detailing how samples were collected and analyzed. This  
144 paper contextualizes this long-term data set so that it can continue to be used to benefit our  
145 collective ecological knowledge of western Lake Erie.

146

147 Table 1. Description of stations sampled in western Lake Erie from 2012 to 2021. Latitude and  
148 longitude (decimal degree) coordinates for each station are target locations as the boat was  
149 allowed to drift at each site during *in-situ* sampling.

150

Station	Latitude	Longitude	Avg. Depth (m)	Years Monitored
WE02	41.762	-83.330	5.4	2012-2021
WE04	41.827	-83.193	8.4	2012-2021
WE06	41.705	-83.385	2.9	2012-2021
WE08	41.834	-83.364	4.8	2012-2021
WE09	41.718	-83.424	2.7	2016-2021
WE12	41.703	-83.254	6.6	2014-2021
WE13	41.741	-83.136	8.9	2014-2021
WE14	41.720	-83.010	9.3	2015
WE15	41.617	-83.009	4.5	2015-2017
WE16	41.660	-83.143	6.2	2018-2021

151



## 152 Methods

### 153 Study Site

154 Based on the lake's bathymetry, Lake Erie can be divided into the eastern, central, and  
155 western basins which in turn influence physical and biological processes (Allinger and Reavie,  
156 2013). The data presented in this paper were collected from the western basin, which  
157 encompasses the western part of the lake to Point Pelee, ON, Canada and Cedar Point, OH,  
158 USA (Fig. 1). The well-mixed western basin is the shallowest (maximum average depth of 11  
159 m), warmest, and most productive of the three basins. Although it's typical for temperate WLE to  
160 have ice cover in the winter (Jan to Mar), summer (Jul to Sep) surface water temperatures often  
161 reach or exceed 25 °C. The western basin receives 95% of its hydraulic inflow from the Detroit  
162 River, which connects Lake Erie hydrologically to Lake Huron via the St. Clair River and Lake  
163 St. Clair (Cousino et al., 2015). Among the other tributaries to WLE (including River Raisin,  
164 Portage River, Ottawa River, Stony Creek, Swan Creek, and Sandusky River), **the Maumee**  
165 **River discharges into the western basin near the city of Toledo, Ohio and contributes a**  
166 **significant amount of sediments and nutrients to the entire Lake Erie basin (Baker et al., 2014a,**  
167 **b). Nutrient and sediment loads from the Maumee River can vary with precipitation, where**  
168 **stormwater runoff can provide a pulse of nutrients into the basin, potentially altering**  
169 **cyanobacteria dynamics (Baker et al., 2014a; King et al., 2022). Land use in the Lake Erie**  
170 **watershed is 75% agricultural and 11% urban, both of which contribute to the large amounts of**  
171 **soluble reactive phosphorus into the basin (Mohamed et al., 2019; Myers et al., 2000).**

172 This dataset includes water quality data from ten monitoring stations on the United  
173 States side of WLE that were sampled from 2012 to 2021 (Figs. 1 & 2, Tables 1 & 2). The  
174 average depth of monitoring stations ranged from 2.7 m at WE9 to 9.3 m at WE14. These sites

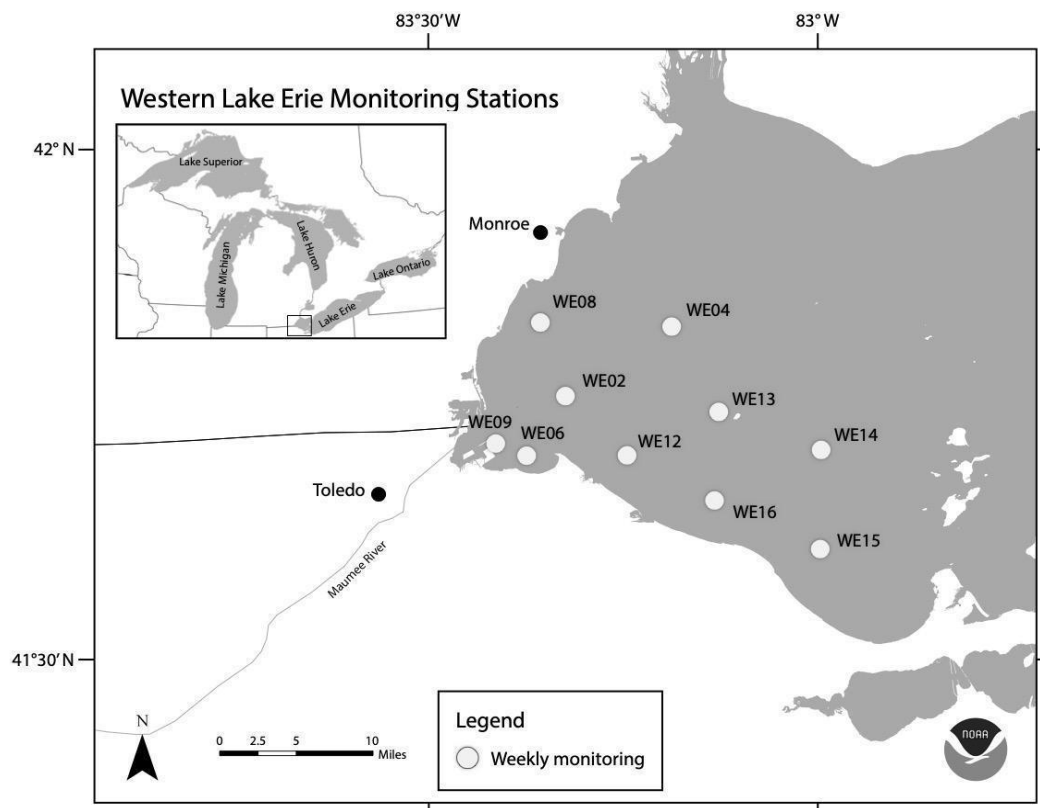




175 were chosen to reflect the various nutrient and hydrologic inputs and gradients into WLE, as  
176 well as represent areas of the basin that are prone to HABs. The Maumee River inflow was a  
177 major consideration in determining these sites. The initial 4 stations sampled in this program  
178 (WE02, WE04, WE06, and WE08) were selected because they were consistently within the  
179 WLE blooms occurring at the time. Additional sites were later added to better represent the  
180 spatial extent of HABs and to augment existing data provided by moored buoy continuous  
181 monitoring systems, advanced monitoring technologies, such as Environmental Sample  
182 Processors (Den Uyl et al., 2022), and other monitoring programs in WLE.

## 183 Field Sampling

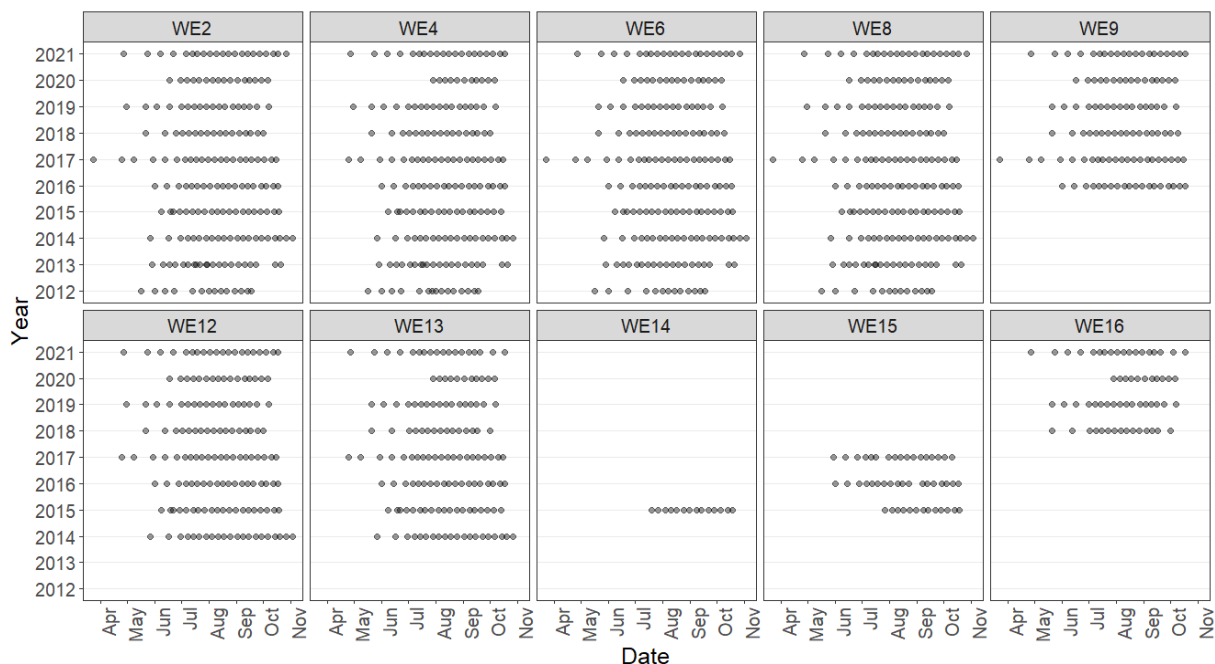
184 Western Lake Erie discrete field sampling was accomplished using NOAA GLERL  
185 research vessels. Sampling took place during ice-free months and aimed to quantify the  
186 environmental conditions prior to, during, and at the end of the bloom (Fig. 2). Sampling stations  
187 represent approximate locations (Table 1; Fig. 1); *in situ* measurements and sampling were  
188 collected once the boat reached the targeted location and then proceeded to drift during  
189 sampling. The frequency and timing of those cruises varied over the first few years but has been  
190 consistent since 2017 (Fig. 2). Sampling was disrupted in 2020 due to the global COVID-19  
191 pandemic and resulting public health restrictions. In 2020, sampling was initiated in mid-June at  
192 a reduced number of sites for select water quality parameters. In July, sampling stations and  
193 parameters were expanded and all stations and parameters were sampled and measured by  
194 August 2020. The prior standard sampling schedule resumed in April 2021.



195

196 Figure 1. Location of western Lake Erie water quality monitoring stations. This map was

197 provided by NOAA for use in this publication.



198

199 Figure 2. Sampling frequency for each monitoring station for years sampled between 2012 to  
 200 2021.

201

202 *In-situ* measurements for conductivity, temperature, dissolved oxygen (DO), beam  
 203 attenuation, transmission, and photosynthetically active radiation (PAR) were taken with a Sea-  
 204 Bird 19plus V2 conductivity, temperature, and depth (CTD) profiler attached to a hydraulic  
 205 crane. Data were collected on the downcast and were reported as the mean of recorded values  
 206 within  $\pm 0.5$  m of the discrete sample depth. In 2012, sample temperature was taken on the boat  
 207 with a Vee Gee Scientific IP67-rated digital thermometer. Sky conditions were recorded at the  
 208 discretion of the field technician at each station during the sampling cruise. A Secchi disk was  
 209 lowered into the water on the shaded side of the boat at each station and the depth at which the  
 210 Secchi disk was no longer visible was recorded (Wetzel and Likens, 2000).

211 Water column samples were collected using a 5 L vertical Niskin bottle (General  
 212 Oceanics model 1010). Niskin casts were evenly distributed between one or more high-density



213 polyethylene bottles that were rinsed with site water and stored in a cooler. Three to four Niskin  
214 casts were used to fill the bottles, such that each bottle is a composite sample of the water  
215 collected. Surface samples were taken 0.75 m below the water's surface, mid-column samples  
216 were taken at approximately 4.25 m below surface, and benthic or bottom samples were taken  
217 at approximately 0.5 m above the lake bottom at each station. Surface samples were taken at  
218 all stations while mid-column and benthic sample collection varied between sites and years.  
219 Scum samples of dense cyanobacterial accumulation on the surface of the water were collected  
220 opportunistically using a 2 L modified Van Dorn water sampler. Sampling times were reported  
221 as Eastern Daylight Time (UT -4:00). Upon arrival at the laboratory, raw water samples were  
222 immediately subsampled and preserved until analysis.

223 Wind speed and wave height data were obtained from moored buoy continuous  
224 monitoring systems in proximity to sampling stations for a timestamp that corresponded to the  
225 time samples were collected at that station. Wave height data for all stations were obtained from  
226 the Toledo Intake Buoy (owned and maintained by Limnotech Inc.). Wind speed data for  
227 stations WE02, WE06, WE09, WE12, WE14, WE15, and WE16 were also collected from this  
228 buoy. Data for this buoy is available through the Great Lakes Observing System (GLOS;  
229 platform ID 45165, <https://seagull.glos.org/data-console/71>). Wind speed data for stations  
230 WE04, WE08, and WE13 were obtained from the Toledo Harbor Light no. 2 buoy (Station  
231 THLO1, owned and maintained by GLERL). Data for this buoy is available through NOAA's  
232 National Data Buoy Center ([https://www.ndbc.noaa.gov/station\\_realtime.php?station=THLO1](https://www.ndbc.noaa.gov/station_realtime.php?station=THLO1)).

233

## 234 Laboratory analysis of samples

235 Water collected from WLE was subsampled to make a range of analytical  
236 measurements in the laboratory (Table 2).



237

238 Table 2. Summary of parameters reported in the dataset.

Parameter	Years monitored	Method
Surface samples	2012-2021	n/a
Mid-column samples	2015	n/a
Benthic samples	2015-2021	n/a
Station depth	2012-2021	Sea-Bird 19plus V2 CTD profiler
Time of sampling (Eastern Daylight Time UT -4:00)	2012-2021	n/a
Latitude (decimal degree)	2012-2021	n/a
Longitude (decimal degree)	2012-2021	n/a
Wind speed (knots)	2015-2021	Moored buoy continuous monitoring systems
Wave height (ft)	2012-2021	Moored buoy continuous monitoring systems
Cloud cover (sky)	2012-2021	n/a
Secchi depth (m)	2012-2021	Wetzel and Likens (2000)
Sample temperature (°C)	2012	Vee Gee Scientific digital thermometer
CTD temperature (°C)	2013-2021	Sea-Bird 19plus V2 CTD profiler
CTD specific conductivity ( $\mu\text{S cm}^{-1}$ )	2013-2021	Sea-Bird 19plus V2 CTD profiler
CTD beam attenuation ( $\text{m}^{-1}$ )	2013-2021	Sea-Bird 19plus V2 CTD profiler
CTD transmission (%)	2013-2021	Sea-Bird 19plus V2 CTD profiler
CTD dissolved oxygen (DO; $\text{mg L}^{-1}$ )	2013-2021	Sea-Bird 19plus V2 CTD profiler
CTD photosynthetically active radiation (PAR; $\mu\text{E m}^{-2} \text{s}^{-1}$ )	2013-2021	Sea-Bird 19plus V2 CTD profiler
Turbidity (NTU)	2013-2021	EPA Method 180.1
Particulate microcystins ( $\mu\text{g L}^{-1}$ )	2012-2021	Wilson et al. (2008)
Dissolved microcystins ( $\mu\text{g L}^{-1}$ )	2014-2021	Wilson et al. (2008)



Phycocyanin ( $\mu\text{g L}^{-1}$ )	2012-2021	Horvath et al. (2013)
Chlorophyll a ( $\mu\text{g L}^{-1}$ )	2012-2021	Speziale et al. (1984)
Total phosphorus (TP; $\mu\text{g L}^{-1}$ )	2012-2021	Standard Method 4500-P
Total dissolved phosphorus (TDP; $\mu\text{g L}^{-1}$ )	2012-2021	Standard Method 4500-P
Soluble reactive phosphorus (SRP; $\mu\text{g L}^{-1}$ )	2012-2021	Standard Method 4500-P
Ammonia ( $\mu\text{g L}^{-1}$ )	2012-2021	Standard Method 4500-nh3-nitrogen (ammonia)
Nitrate + Nitrite ( $\text{mg L}^{-1}$ )	2012-2021	Standard Method 4500-no3-nitrogen (nitrate)
Urea ( $\mu\text{g L}^{-1}$ )	2016-2017	Milvenna and Savidge (1992), Goeyens et al. (1998), Chaffin and Bridgeman (2014)
Particulate organic carbon (POC; $\text{mg L}^{-1}$ )	2012-2021	Hedges and Stern (1984)
Particulate organic nitrogen (PON; $\text{mg L}^{-1}$ )	2012-2021	Hedges and Stern (1984)
Colored dissolved organic material (CDOM; $\text{m}^{-1}$ )	2014-2021	Binding et al. (2008), Mitchell et al. (2003)
Dissolved organic carbon (DOC; $\text{mg L}^{-1}$ )	2012-2017	APHA Standard Method 5310 B
Total suspended solids (TSS; $\text{mg L}^{-1}$ )	2012-2021	APHA Standard Method 2540
Volatile suspended solids (VSS; $\text{mg L}^{-1}$ )	2012-2021	APHA Standard Method 2540

239

## 240 Optical properties

241 Turbidity was measured on raw samples using a Hach 2100AN Turbidimeter following  
 242 US EPA method 180.1 (1993). Colored dissolved organic material (CDOM, also defined as  
 243 chromophoric dissolved organic matter) was determined by filtering lake water through an acid  
 244 rinsed  $0.2 \mu\text{m}$  nuclepore polycarbonate filter into acid-washed and combusted borosilicate vials.  
 245 Optical density of the filtered samples was then measured using a Perkin Elmer UV/VIS



246 Lambda 35 spectrophotometer at wavelengths from 300-800 nm. CDOM absorption was  
247 calculated at 400 nm (Mitchell et al., 2003; Binding et al., 2008).

248 Dissolved organic carbon (DOC) concentrations were determined following American  
249 Public Health Association (APHA) Standard Method 5310 B. Briefly, lake water was filtered  
250 through 0.45  $\mu\text{m}$  polyvinylidene difluoride membrane filters into combusted borosilicate glass  
251 vials and frozen at  $-20^{\circ}\text{C}$  until analysis. The filtrate was acidified with HCl and sparged with air  
252 for 6 min before being analyzed on a Shimadzu total organic carbon analyzer.

253 Duplicate samples for particulate organic carbon (POC) and particulate organic nitrogen  
254 (PON) were collected onto pre-combusted glass fiber filters and analyzed following Hedges and  
255 Stern (1984) Samples were stored at  $-20^{\circ}\text{C}$  until analysis. The filters were then acidified by  
256 fumigation with 10% HCl and dried at  $70^{\circ}\text{C}$  for 24 h before being quantified on a Perkin Elmer  
257 2400 or a Carlo-Erba 1110 CHN elemental analyzer.

258 Total suspended solids (TSS) and volatile suspended solids (VSS) were determined via  
259 gravimetric analysis following APHA Standard Method 2540. A known volume of lake water was  
260 filtered through a pre-combusted, pre-weighed Whatman GF/F glass fiber filter. The filters were  
261 then dried at  $60^{\circ}\text{C}$  for at least 24 h and reweighed. The difference in mass between the pre-  
262 weighed and processed filter was reported as TSS. Volatile suspended solids concentrations  
263 were quantified by combusting the filters used for TSS analysis at  $450^{\circ}\text{C}$  for 4 h, weighing the  
264 combusted filters, and calculating the mass lost.

## 265 Nutrient fractions

266 Total phosphorus (TP) and total dissolved phosphorus (TDP) samples were collected in  
267 duplicate by subsampling 50 mL (2012 to 2019) or 20 mL (2020 to 2021) of lake water into acid  
268 washed glass tubes and by filtering 20 mL of lake water through a 0.2  $\mu\text{m}$  membrane filter and  
269 collecting the filtrate, respectively. Samples for TP and TDP were refrigerated until samples  
270 were digested with potassium persulfate solution and autoclaved at  $121^{\circ}\text{C}$  for 30 min, modified



271 from APHA Standard Method 4500-P. Digested TP and TDP samples were stored at room  
272 temperature until concentrations were measured on a Seal QuAAtro continuous segmented flow  
273 analyzer (SEAL Analytical Inc.) from 2012 to 2019 and a Seal AA3 from 2020 to 2021 using the  
274 ascorbic acid molybdenum method as detailed by the instrument manual and APHA Standard  
275 Method 4500-P. Analytical detection limits for the analyses were taken from the instrument  
276 manufacturer's documentation.

277 Soluble reactive phosphorus (SRP), ammonia, nitrate + nitrite, and urea were each  
278 determined by filtering 12 mL of lake water through a 0.2 µm membrane filter into 15 mL  
279 centrifuge tubes during field sampling. Sample filtrates were stored at -20 °C upon receipt at the  
280 laboratory. Soluble reactive phosphorus, ammonia, and nitrate + nitrite concentrations were  
281 determined simultaneously on a Seal AA3 continuous segmented flow analyzer. Soluble  
282 reactive phosphorus concentrations, like TP and TDP concentrations, were measured using the  
283 ascorbic acid molybdenum method as detailed by the instrument manual and APHA Standard  
284 Method 4500-P. Ammonia concentrations were measured using Bertholet reactions according  
285 to the instrument manual and APHA Standard Method 4500-nh3-nitrogen. Nitrate + nitrite  
286 concentrations were measured using copper-cadmium reduction methods according to the  
287 instrument manual and APHA Standard Method 4500-no3-nitrogen. Analytical detection limits  
288 for these inorganic nutrient analyses were taken from the instrument manufacturer's  
289 documentation. Urea samples were measured by adding diacetyl monoxime and  
290 thiosemicarbazide to the filtrate and briefly vortexing to mix, followed by adding sulfuric acid and  
291 ferric chloride to the solution and briefly vortexing to mix. Samples were then incubated in the  
292 dark for 72 h at room temperature before absorbance at 520 nm was read on a Perkin Elmer  
293 UV/VIS Lambda 35 spectrophotometer. Urea concentrations were then quantified using a  
294 standard curve (Mulvenna and Savidge, 1992; Goeyens et al., 1998; Chaffin and Bridgeman,  
295 2014). The detection limit was calculated using the standard deviation of repeated  
296 measurements.





## 297 Pigments and microcystins

298 Particulate phycocyanin and chlorophyll *a* concentrations were determined by filtering a  
299 known volume of lake water under low vacuum (<200 mm Hg) onto 47 mm Whatman GF/F  
300 glass fiber filters (Cytiva Life Sciences). Particulate phycocyanin sample filters were stored in 15  
301 mL conical polypropylene centrifuge tubes and chlorophyll *a* sample filters were stored in amber  
302 glass vials at -20 °C until analysis. Analysis methods for particulate phycocyanin were derived  
303 from Horváth et al. (2013) where 9 mL of phosphate buffer was added to sample tubes and samples  
304 were agitated using a shaker at 5 °C for 15 min at 100 rpm then vortexed for 10 s each. To  
305 encourage cell lysis, samples were subjected to three freeze/thaw cycles at -20 °C followed by  
306 sonication for 20 min using a Fisher FS110 H sonicator. Fluorescence of the extracted samples was  
307 measured using an Aquafluor 8000-010 fluorometer (Turner Designs) with excitation from 400-600  
308 nm and emission filter of >595 nm. Particulate phycocyanin was calibrated annually against C-  
309 Phycocyanin material from Sigma-Aldrich. Analysis methods for chlorophyll *a* were derived from  
310 Speziale et al. (1984) where chlorophyll *a* was extracted from samples using dimethylformamide  
311 and placed into a 65 °C water bath for 15 min. Samples were then cooled to room temperature  
312 and vortexed for 15-20 s before being quantified using a 10 AU fluorometer (Turner Designs)  
313 with excitation filter of 436 nm and emission at 680 nm. Phycocyanin and chlorophyll *a*  
314 procedures were performed under low or green light to reduce pigment degradation ~~within the cell.~~

315 Dissolved and particulate microcystins were quantified using a procedure adapted from  
316 Wilson et al. (2008). Dissolved microcystins (dMC) were determined through duplicate samples  
317 of ~ 2 mL filtrate that was passed through a 0.2 µm membrane filter and stored in glass vials at -  
318 20 °C until analysis. Particulate microcystins (pMC) were collected by filtering a known volume  
319 of lake water onto a Whatman GF/F glass fiber filter (2012 to 2015) or a 3 µm pore size  
320 polycarbonate membrane filter (2016 to 2021). Particulate MC was then extracted from the  
321 filters. In sampling years 2012 to 2015, glass fiber filters were submerged in a glass vial



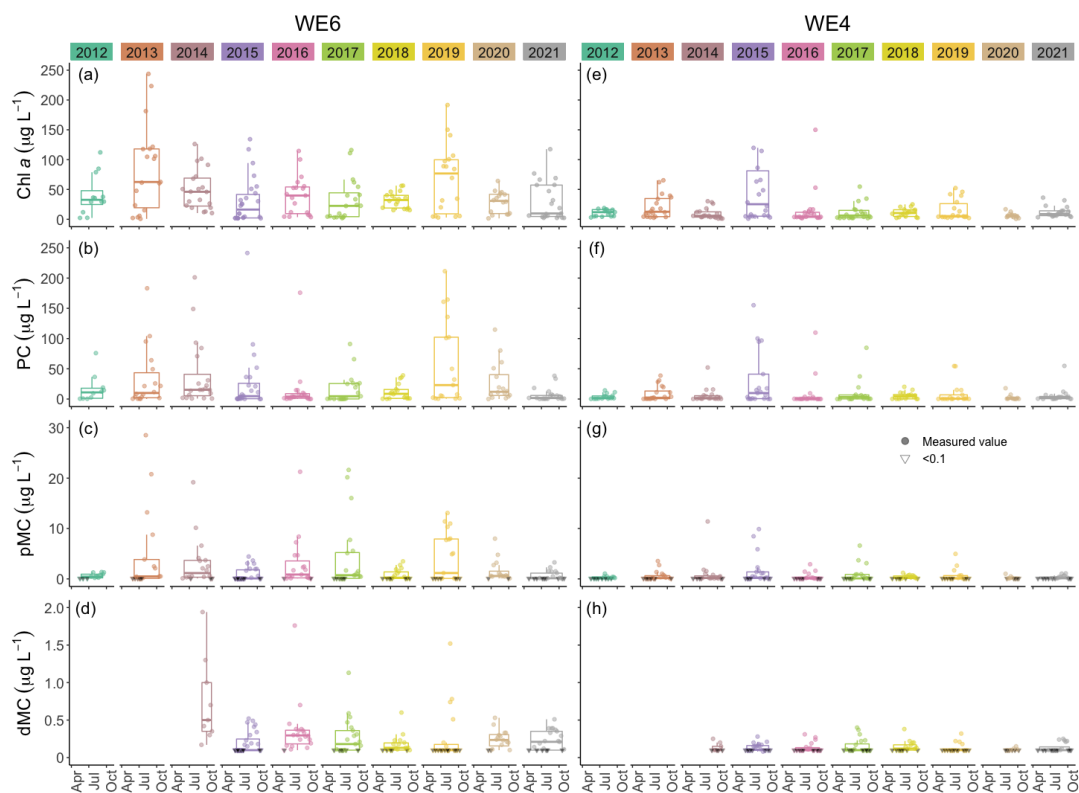
322 containing a 75:25 methanol:water solution (MeOH/H<sub>2</sub>O) and sonicated in an ice bath for 2 min.  
323 The samples were centrifuged for 15 min and the supernatant was transferred to a clean glass  
324 vial. An additional 5 mL of MeOH/H<sub>2</sub>O was added to the filter/precipitate and the sample was  
325 incubated at -20 °C for 5 h. The sample was then sonicated for 2 min, centrifuged, and the  
326 supernatant was removed and added to the first extract vial. The composite supernatant was  
327 then centrifuged under a vacuum until dry. The dried extract was then stored at -20 °C until  
328 analysis. Particulate MC concentrations were then determined by adding 1 mL of MilliQ water to  
329 the sample and using sonication to dissolve the dried extract. For sampling years 2016 to 2021,  
330 filters were stored in 2 mL sterile microcentrifuge tubes at -20 °C until analysis. During analysis,  
331 pMC were extracted from the membrane filters by adding 1 mL of MilliQ water and subjecting  
332 samples to three freeze/thaw cycles at -20 °C followed by addition of Abraxis QuickLyse  
333 reagents according to the manufacturer (Eurofins/Abraxis). Particulate MC samples for all  
334 sampling years were analyzed immediately after extraction. For all sampling years, dMC and  
335 pMC concentrations were determined using a congener-independent enzyme-linked  
336 immunosorbent assay (ELISA) kit designed to detect and quantify microcystins and nodularins  
337 using the ADDA moiety (Envirologix brand used from 2012 to 2015; Eurofins/Abraxis  
338 microcystins/nodularins (ADDA) (EPA ETV) (EPA method 546), ELISA, 96-test kit used from  
339 2016 to 2021). Analytical detection limits for the analyses were taken from the manufacturer's  
340 documentation.



## 341 Results and Discussion

342 This dataset demonstrates the temporal and spatial variability in water quality  
343 parameters in western Lake Erie from 2012 to 2021. Overall, sites **closer** to the Maumee River  
344 inflow (i.e., WE06 and WE09) had the highest median concentrations of nutrients, sediments,  
345 pigments, and microcystins compared to sites further out in the basin (i.e., WE02, WE04, and  
346 WE13; Table 3). Stations WE06 and WE04 were sampled since the initiation of the monitoring  
347 program and consistently represented the high and low extremes of water quality observations  
348 during a given time point, respectively, (Table 3) and select parameters for these two sites are  
349 represented in figs. 3 and 4. Supplemental figs. 1-16 display the same parameters as figs. 3 and  
350 4 for the remaining stations.

351



352

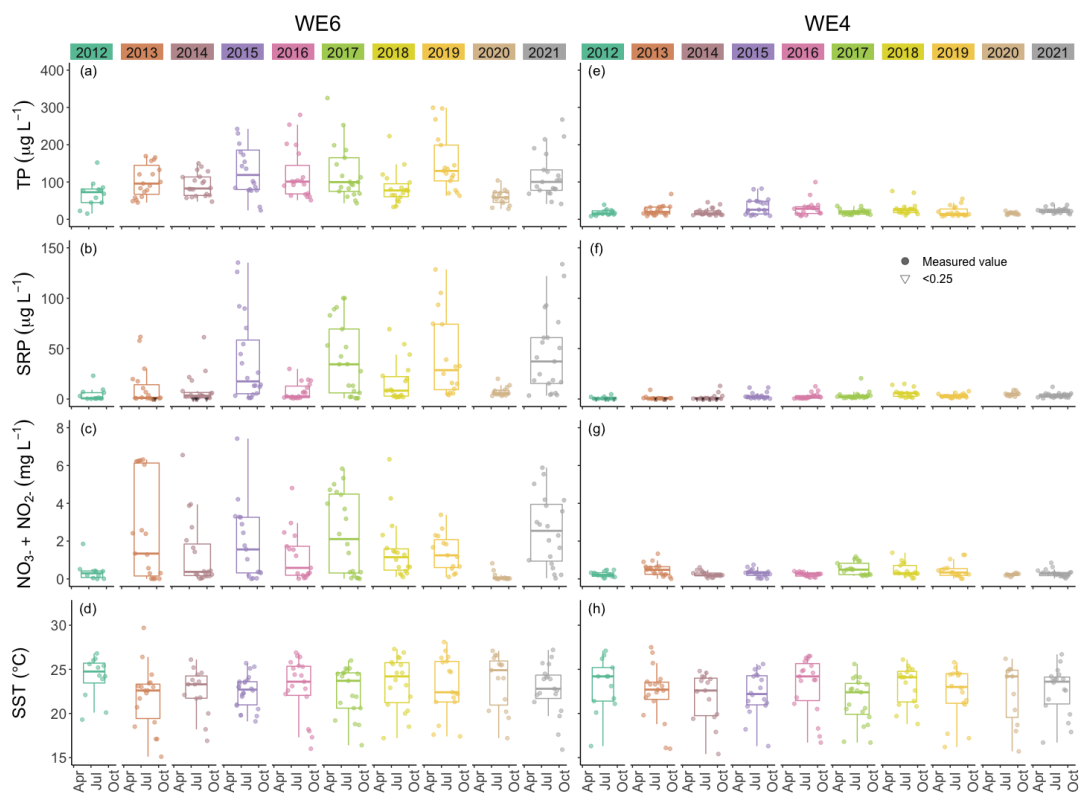
353 Fig 3. Comparison of chlorophyll a (Chl a), phycocyanin (PC), particulate microcystins (pMC),  
354 and dissolved microcystins (dMC) between stations WE04 and WE06 from 2012 to 2021.

355 Boxplots represent the median and 25% and 75% quartiles with whiskers extending to the

356 highest or lowest point within 1.5x the interquartile range. A scatterplot is overlaid on the

357 boxplots.

358



359

360 Fig 4. Comparison of total phosphorus (TP), soluble reactive phosphorus (SRP), nitrate plus  
361 nitrite ( $\text{NO}_3^- + \text{NO}_2^-$ ), and sea surface temperature (SST) between stations WE04 and WE06  
362 from 2012 to 2021. Boxplots represent the median and 25% and 75% quartiles with whiskers  
363 extending to the highest or lowest point within 1.5x the interquartile range. A scatterplot is  
364 overlaid on the boxplots.

365



366 Table 3. Median values of each parameter at each monitoring station for all surface samples  
 367 collected between 2012 to 2021.

Secchi depth (m)	Temp. (°C)	Cond. (µS cm)	DO (mg L <sup>-1</sup> )	PAR (µE m <sup>-2</sup> s <sup>-1</sup> )	Beam Attenuation (m)	Transmission (%)	Turbidity (NTU)	Particulate TIC (µg L <sup>-1</sup> )	Dissolved TIC (µg L <sup>-1</sup> )	Phycoerythrin (µg L <sup>-1</sup> )	Chl-a (µg L <sup>-1</sup> )	TP (µg L <sup>-1</sup> )	TDP (µg L <sup>-1</sup> )	SRP (µg L <sup>-1</sup> )	Ammonia (µg L <sup>-1</sup> )	Nitrate + Nitrite (mg L <sup>-1</sup> )	POC (mg L <sup>-1</sup> )	PON (mg L <sup>-1</sup> )	CDOM (m)
WE02 0.8	23.1	287	7.7	264	5.1	28.2	9.9	0.78	0.20	4.8	17.5	53.3	12.8	5.7	12.6	0.44	1.4	0.23	0.99
WE04 2.0	22.9	244	7.6	377	2.2	58.4	3.0	0.46	0.17	1.2	7.7	19.2	4.5	2.2	12.9	0.27	0.63	0.10	0.34
WE06 0.5	23.0	346	7.6	173	6.4	20.5	14.8	1.5	0.28	8.0	33.0	90.1	18.7	8.7	11.8	0.83	2.4	0.38	2.0
WE08 1.0	23.3	299	7.7	166	4.3	34.4	9.0	0.88	0.22	5.7	19.5	50.9	12.3	5.8	13.8	0.45	1.5	0.25	1.1
WE09 0.3	23.9	395	7.1	127	12.6	4.3	23.2	0.95	0.26	5.2	32.6	133	44.8	29.5	43.1	1.4	2.5	0.42	2.4
WE12 0.8	23.1	276	7.7	266	5.4	25.9	11.0	0.67	0.16	2.9	15.1	47.6	10.1	5.4	8.4	0.31	1.2	0.20	0.81
WE13 1.5	22.9	244	7.8	456	2.7	52.4	4.3	0.56	0.15	2.6	8.6	22.3	5.0	2.7	10.2	0.25	0.78	0.14	0.38
WE14 1.4	23.2	238	8.1	796	3.7	40.2	7.2	0.80	0.16	17.0	40.0	31.0	4.7	1.5	2.9	0.17	1.7	0.27	0.60
WE15 1.0	23.0	261	7.7	391	3.4	43.0	6.3	0.86	0.19	2.7	12.7	34.8	5.5	2.0	23.9	0.27	1.1	0.18	0.54
WE16 1.3	24.1	269	7.4	297	3.6	40.8	6.3	0.91	0.18	3.4	12.3	30.2	7.2	4.0	10.6	0.30	1.0	0.16	0.71

368



## 369 Physicochemical properties

370 Median surface temperatures for all samples across all years ranged from 22.9 to 24.1  
371 °C and median benthic temperatures ranged from 22.8 to 23.2 °C (Table 3, Fig. 4), indicating  
372 that WLE was thermally well mixed throughout the sampling period. A summary of the dataset  
373 indicates that 23.8% of surface temperatures were  $\geq 25$  °C, and these higher temperatures all  
374 occurred from mid-June through the end of September. Bloom forming cyanobacteria species in  
375 Lake Erie, including *Microcystis spp.*, often reach maximum growth rates at warmer  
376 temperatures ( $\geq 25$  °C) than eukaryotic phytoplankton (Steffen et al., 2014; Huisman et al.,  
377 2018). Despite having warmer temperatures that promote recurring HABs, there was only one  
378 recorded instance of hypoxia ( $DO < 2$  mg L<sup>-1</sup>) in the dataset and it occurred at WE13 on 08 July  
379 2019. Median DO was 7.62 mg L<sup>-1</sup> in all surface samples and 7.02 mg L<sup>-1</sup> in all benthic samples  
380 from 2012 to 2021 (Table 3), again indicating minimal stratification in WLE during sampling.  
381 Median conductivity from 2012 to 2021 was highest at sites WE06 and WE09, which are closest  
382 to the Maumee River input, and lowest at sites WE04 and WE13 near the middle of the basin  
383 (Table 3). WE06 and WE09 were the only sites to have median conductivity values above 300  
384  $\mu\text{S cm}^{-1}$ .

## 385 Optical properties

386 Biotic and abiotic particulate concentrations and movement patterns in WLE are prone to  
387 spatial and seasonal variations and are heavily influenced by loading from the Maumee River  
388 (Prater et al., 2017; Maguire et al., 2022). Secchi depth, turbidity, and PAR measurements have  
389 been correlated with distance from Maumee Bay, where light penetration was lowest near the  
390 Maumee River (Chaffin et al., 2011). Variability in optical property measurements in WLE is also  
391 dependent on Maumee River inputs, and changes in optical properties can potentially be used



392 in remote sensing algorithms to detect changes in water quality (Sayers et al., 2019). Median  
393 Secchi disk depth over the entire dataset was highest at WE04 and lowest at WE06 and WE09,  
394 which are closest to the Maumee River (Table 3). Other optical properties, such as PAR, beam  
395 attenuation, and transmittance also followed this spatial pattern. In a summary of all samples,  
396 median PAR measured at 0.5 m below surface was highest at WE13 and WE14 and lowest at  
397 WE09; median transmittance was highest at WE04 and lowest at WE09; and median beam  
398 attenuation and turbidity were highest at WE09 and lowest at WE04 (Table 3). Median turbidity  
399 values at each site over the 2012 to 2021 period were within the range of previously reported  
400 values in the WLE basin (Barbiero and Tuchman, 2004). Median CDOM absorbance and DOC,  
401 TSS, and VSS concentrations were again highest at WE09 and lowest at WE04 (Table 3).  
402 CDOM gradients in WLE are likewise affected by loading from the Maumee River (Cory et al.,  
403 2016) and DOC and CDOM values from this dataset have been used as predictor variables in  
404 models estimating PAR attenuation variation in WLE (Weiskerger et al., 2018).

## 405 Nutrient fractions

406 The Maumee River is a major contributor of nutrients to Lake Erie (Steffen et al., 2014;  
407 Kast et al., 2021). Median TP concentrations in WLE from 2012 to 2021 were lowest at WE04  
408 and highest at WE09 (Table 3, Fig. 4). Median concentrations at each station from 2012 to 2021  
409 were above the GLWQA Annex 4 goals for TP concentration in open waters, which is  $15 \mu\text{g P L}^{-1}$   
410 for WLE. This goal was met in 92 of 1275 (7.2%) samples and these target values were  
411 primarily recorded from stations WE04 and WE13. Sites closer to the mouth of the Maumee  
412 River had higher median TP values. While TP loading from the Maumee River tributary declined  
413 between 1982 to 2018 (Rowland et al., 2020) the proportion of dissolved P has increased  
414 (Joosse and Baker, 2011; Stow et al., 2015). Median TDP values in the WLE dataset were  
415 lowest at WE04 and highest at WE09 (Table 3) with a highest recorded value of  $274 \mu\text{g P L}^{-1}$  at





416 WE08 in 2015. Median SRP concentrations for each station in this dataset were lowest at WE14  
417 and WE15 and were highest at WE09 (Table 3). The maximum recorded SRP concentration  
418 was  $135.4 \mu\text{g P L}^{-1}$  at WE06 in 2015 (Fig. 4). Using this dataset, Newell et al. (2019) found that  
419 the Maumee River N loading has become more chemically reduced over time where ammonium  
420 and PON have increased. Median ammonia concentrations in WLE from 2012 to 2019 were  
421 lowest at WE12 and WE14 and highest at WE09 (Table 3) with a recorded maximum  
422 concentration of  $2109 \mu\text{g N L}^{-1}$  at WE12 in 2017. Median nitrate + nitrite was lowest at WE13  
423 and WE14 and highest at WE09 (Table 3), with a maximum recorded value of  $9.5 \text{ mg N L}^{-1}$  at  
424 WE09 in 2016. See Fig. 4 for a comparison of nitrate + nitrite concentrations between WE04  
425 and WE06. Median PON concentrations were lowest at WE04 and highest at WE09 (Table 3)  
426 with a recorded max of  $40.93 \text{ mg N L}^{-1}$  at WE08 in 2015.

## 427 Pigments and microcystins

428 Median extracted chlorophyll *a* concentrations in surface waters from 2012 to 2021 were  
429 lowest at WE04 and highest at WE06 (Table 3, Fig. 3). The highest recorded surface  
430 concentration of chlorophyll *a* was  $6784 \mu\text{g L}^{-1}$  on 10 August 2015 at WE08 during the most  
431 severe bloom year in this dataset, according to the CI Index (Wynne et al., 2013; Lunetta et al.,  
432 2015). The highest measured levels of particulate phycocyanin, pMC, and TP were also  
433 recorded at WE06 on 10 August 2015. Other notably high chlorophyll *a* concentrations were  
434 measured during severe bloom years in 2017 ( $532 \mu\text{g L}^{-1}$  at WE09 on 04 August) and 2019 ( $593$   
435  $\mu\text{g L}^{-1}$  at WE09 on 05 August). Similarly, median surface particulate phycocyanin concentration  
436 for 2012 to 2021 was highest at WE06 and lowest at WE04 (Table 3, Fig. 4). The highest  
437 recorded phycocyanin value was from WE08 on 10 August 2015 ( $8228 \mu\text{g L}^{-1}$ ), followed by  $3315$   
438  $\mu\text{g L}^{-1}$  at WE06 in 2013 during another severe bloom year.



439 Particulate MC concentrations had highest median concentrations at WE06 and were  
440 lowest at WE04 (Table 3, Fig. 4), similar to particulate chlorophyll *a* and phycocyanin  
441 observations. The highest recorded particulate MC concentration in this dataset was from 10  
442 August 2015 at WE08 during a severe bloom year ( $297 \mu\text{g L}^{-1}$ ), followed by  $289 \mu\text{g L}^{-1}$  at WE06  
443 in 2017 during another severe bloom year according to the CI Index (Wynne et al., 2013;  
444 Lunetta et al., 2015). Median dMC concentrations were highest at WE06 and lowest at WE13  
445 (Table 3). The maximum dissolved MC in the dataset was  $8.19 \mu\text{g L}^{-1}$  at WE09 on 05 August  
446 2019, which correlates with high chlorophyll *a* concentrations.

447 Although the United States does not federally enforce water quality criteria or regulations  
448 for cyanotoxins in drinking water, the US EPA has a recommended health advisory of  $1.6 \mu\text{g L}^{-1}$   
449 microcystins in drinking water for school-age children through adults (US EPA, 2015) while the  
450 WHO and the Ohio EPA use  $1 \mu\text{g L}^{-1}$  microcystins as a guideline (WHO, 2020). From 2012 to  
451 2021, 44.4% of pMC samples in this dataset exceeded the WHO guidelines and 34.1%  
452 exceeded the US EPA health advisory. Monitoring MC concentrations in western Lake Erie has  
453 become especially pertinent since August 2014 when the Toledo, OH drinking water treatment  
454 plant was contaminated with microcystins in excess of  $1 \mu\text{g L}^{-1}$  and customers were alerted to  
455 not drink their tap water until toxin levels were decreased (Steffen et al., 2017). The pMC  
456 concentrations at our WLE monitoring stations varied from  $1.2\text{-}10.1 \mu\text{g L}^{-1}$  on 04 August 2014  
457 during this crisis.

458



## 459 Data Availability

460 The entire dataset detailed in this manuscript can be freely accessed through the NOAA  
461 National Centers for Environmental Information (NCEI) data repository at  
462 <https://www.ncei.noaa.gov/>. The data collection is titled “Physical, chemical, and biological water  
463 quality monitoring data to support detection of Harmful Algal Blooms (HABs) in western Lake  
464 Erie, collected by the Great Lakes Environmental Research Laboratory and the Cooperative  
465 Institute for Great Lakes Research since 2012”. The digital object identifier is  
466 <https://doi.org/10.25921/11da-3x54>. The data presented in this manuscript are available in three  
467 separate accession files within this collection including: 2012 to 2018 data is available under  
468 NCEI Accession 0187718 v2.2 at <https://www.ncei.noaa.gov/archive/accession/0187718>; 2019  
469 data is available under NCEI Accession 0209116 v1.1 at  
470 <https://www.ncei.noaa.gov/archive/accession/0209116>; 2020 to 2021 data is available under  
471 NCEI Accession 0254720 v1.1 at <https://www.ncei.noaa.gov/archive/accession/0254720>  
472 (Cooperative Institute for Great Lakes Research, University of Michigan; NOAA Great Lakes  
473 Environmental Research Laboratory, 2019). Future data will be added to this collection as it  
474 becomes available.



## 475 Conclusions

476           The western Lake Erie data collected and compiled by NOAA GLERL and CIGLR  
477 represent ten years of routine water quality monitoring to detect, track, and predict  
478 cyanobacterial HAB events in an area of the Great Lakes that has experienced significant  
479 environmental degradation. While this monitoring initiative started in conjunction with remote  
480 sensing efforts, it eventually became a standalone program. This ongoing program provides a  
481 service to the region and contributes data for investigating the nuanced dynamics of potentially  
482 toxic HABs fueled by excess nutrient loading into the WLE basin. For instance, this dataset has  
483 assisted in assessing progress toward binational nutrient loading reduction efforts on lake basin  
484 concentrations of phosphorus. Long-term monitoring programs like this one provide consistent  
485 data which is useful for identifying patterns and variations within the ecosystem and in  
486 determining the root cause of those changes. As the sites and parameters of this monitoring  
487 program have already changed to adapt to the needs of research, this program will continue to  
488 evolve as we consider adding parameters that encompass other aspects of bloom dynamics.  
489 For example, lake samples can be analyzed for genomic data that will provide insights on the  
490 ability of the current phytoplankton community to produce microcystins. This decadal history has  
491 already been an invaluable resource for the research community, and it will continue to enrich  
492 our collective scientific knowledge of water quality dynamics in western Lake Erie.

493



## 494 Acknowledgements

495 Funding was awarded to the Cooperative Institute for Great Lakes Research (CIGLR) through  
496 the NOAA Cooperative Agreement with the University of Michigan (NA17OAR4320152 and  
497 NA22OAR4320150). This is CIGLR contribution number ##### and NOAA-GLERL contribution  
498 #####. The GLERL/CIGLR monitoring program was supported by the Great Lakes Restoration  
499 Initiative. We thank Gabrielle Farina for preparing Fig. 1.

500

501



## 502 Author Contributions

503 Anna G Boegehold prepared the manuscript. Ashley M. Burtner performed field sampling,  
504 laboratory processing, data processing, QA/QC and data management, manuscript revision,  
505 data curation. Andrew Camilleri performed field sampling, laboratory processing, manuscript  
506 revision. Glenn Carter performed field sampling, laboratory processing, data processing,  
507 methodology. Paul DenUyl performed field sampling, laboratory processing, manuscript  
508 revision. David Fanslow performed field sampling, laboratory processing. Deanna Fyffe  
509 Semenyuk performed field sampling, laboratory processing, manuscript revision. Casey Godwin  
510 was responsible for project administration, supervision, visualization, manuscript revision,  
511 methodology, field sampling, sample processing. Duane Gossiaux performed field sampling,  
512 laboratory processing, manuscript revision, methodology. Tom Johengen was responsible for  
513 project administration, supervision, field sampling, methodology. Holly Kelchner performed field  
514 sampling, laboratory processing, manuscript revision. Christine Kitchens performed field  
515 sampling, laboratory processing, data processing, manuscript revision. Lacey A. Mason was  
516 responsible for data curation, manuscript revision. Kelly McCabe performed field sampling,  
517 laboratory processing, manuscript revision, methodology. Danna Palladino performed field  
518 sampling, laboratory processing, data processing, manuscript revision. Dack Stuart performed  
519 field sampling, data processing. Henry Vanderploeg was responsible for project administration,  
520 supervision. Reagan Errera was responsible for project administration, supervision,  
521 Visualization, manuscript revision, methodology.

522



## 523 Competing Interests

524 The authors declare that they have no conflict of interest



## 525 References

- 526 Allinger, L. E. and Reavie, E. D.: The ecological history of Lake Erie as recorded by the  
527 phytoplankton community, *J. Gt. Lakes Res.*, 39, 365–382,  
528 <https://doi.org/10.1016/j.jglr.2013.06.014>, 2013.
- 529 Avouris, D. M. and Ortiz, J. D.: Validation of 2015 Lake Erie MODIS image spectral  
530 decomposition using visible derivative spectroscopy and field campaign data, *J. Gt. Lakes Res.*,  
531 45, 466–479, <https://doi.org/10.1016/j.jglr.2019.02.005>, 2019.
- 532 Baker, D. B., Ewing, D. E., Johnson, L. T., Kramer, J. W., Merryfield, B. J., Confesor, R. B.,  
533 Peter Richards, R., and Roerdink, A. A.: Lagrangian analysis of the transport and processing of  
534 agricultural runoff in the lower Maumee River and Maumee Bay, *J. Gt. Lakes Res.*, 40, 479–  
535 495, <https://doi.org/10.1016/j.jglr.2014.06.001>, 2014a.
- 536 Baker, D. B., Confesor, R., Ewing, D. E., Johnson, L. T., Kramer, J. W., and Merryfield, B. J.:  
537 Phosphorus loading to Lake Erie from the Maumee, Sandusky and Cuyahoga rivers: The  
538 importance of bioavailability, *J. Gt. Lakes Res.*, 40, 502–517,  
539 <https://doi.org/10.1016/j.jglr.2014.05.001>, 2014b.
- 540 Barbiero, R. P. and Tuchman, M. L.: Long-term Dreissenid Impacts on Water Clarity in Lake  
541 Erie, *J. Gt. Lakes Res.*, 30, 557–565, [https://doi.org/10.1016/S0380-1330\(04\)70371-8](https://doi.org/10.1016/S0380-1330(04)70371-8), 2004.
- 542 Berry, M. A., Davis, T. W., Cory, R. M., Duhaime, M. B., Johengen, T. H., Kling, G. W., Marino,  
543 J. A., Den Uyl, P. A., Gossiaux, D., Dick, G. J., and Deneff, V. J.: Cyanobacterial harmful algal  
544 blooms are a biological disturbance to Western Lake Erie bacterial communities, *Environ.*  
545 *Microbiol.*, 19, 1149–1162, <https://doi.org/10.1111/1462-2920.13640>, 2017.
- 546 Bertani, I., Steger, C. E., Obenour, D. R., Fahnenstiel, G. L., Bridgeman, T. B., Johengen, T. H.,  
547 Sayers, M. J., Shuchman, R. A., and Scavia, D.: Tracking cyanobacteria blooms: Do different  
548 monitoring approaches tell the same story?, *Sci. Total Environ.*, 575, 294–308,  
549 <https://doi.org/10.1016/j.scitotenv.2016.10.023>, 2017.
- 550 Binding, C. E., Jerome, J. H., Bukata, R. P., and Booty, W. G.: Spectral absorption properties of  
551 dissolved and particulate matter in Lake Erie, *Remote Sens. Environ.*, 112, 1702–1711,  
552 <https://doi.org/10.1016/j.rse.2007.08.017>, 2008.
- 553 Bosse, K. R., Sayers, M. J., Shuchman, R. A., Fahnenstiel, G. L., Ruberg, S. A., Fanslow, D. L.,  
554 Stuart, D. G., Johengen, T. H., and Burtner, A. M.: Spatial-temporal variability of in situ  
555 cyanobacteria vertical structure in Western Lake Erie: Implications for remote sensing  
556 observations, *J. Gt. Lakes Res.*, 45, 480–489, <https://doi.org/10.1016/j.jglr.2019.02.003>, 2019.
- 557 Bridoux, M., Sobiechowska, M., Perez-Fuentetaja, A., and Alben, K. T.: Algal pigments in Lake  
558 Erie dreissenids, pseudofeces and sediments, as tracers of diet, selective feeding and  
559 bioaccumulation, *J. Gt. Lakes Res.*, 36, 437–447, <https://doi.org/10.1016/j.jglr.2010.06.005>,  
560 2010.
- 561 Buratti, F. M., Manganelli, M., Vichi, S., Stefanelli, M., Scardala, S., Testai, E., and Funari, E.:  
562 Cyanotoxins: producing organisms, occurrence, toxicity, mechanism of action and human health





- 563 toxicological risk evaluation, *Arch. Toxicol.*, 91, 1049–1130, <https://doi.org/10.1007/s00204-016-1913-6>, 2017.  
564
- 565 Carmichael, W. W. and Boyer, G. L.: Health impacts from cyanobacteria harmful algae blooms:  
566 Implications for the North American Great Lakes, *Harmful Algae*, 54, 194–212,  
567 <https://doi.org/10.1016/j.hal.2016.02.002>, 2016.
- 568 Chaffin, J. D. and Bridgeman, T. B.: Organic and inorganic nitrogen utilization by nitrogen-  
569 stressed cyanobacteria during bloom conditions, *J. Appl. Phycol.*, 26, 299–309,  
570 <https://doi.org/10.1007/s10811-013-0118-0>, 2014.
- 571 Chaffin, J. D., Bridgeman, T. B., Heckathorn, S. A., and Mishra, S.: Assessment of *Microcystis*  
572 growth rate potential and nutrient status across a trophic gradient in western Lake Erie, *J. Gt.*  
573 *Lakes Res.*, 37, 92–100, <https://doi.org/10.1016/j.jglr.2010.11.016>, 2011.
- 574 Charlton, M. N., Milne, J. E., Booth, W. G., and Chiocchio, F.: Lake Erie Offshore in 1990:  
575 Restoration and Resilience in the Central Basin, *J. Gt. Lakes Res.*, 19, 291–309,  
576 [https://doi.org/10.1016/S0380-1330\(93\)71218-6](https://doi.org/10.1016/S0380-1330(93)71218-6), 1993.
- 577 Conroy, J. D., Kane, D. D., Dolan, D. M., Edwards, W. J., Charlton, M. N., and Culver, D. A.:  
578 Temporal Trends in Lake Erie Plankton Biomass: Roles of External Phosphorus Loading and  
579 Dreissenid Mussels, *J. Gt. Lakes Res.*, 31, 89–110, [https://doi.org/10.1016/S0380-1330\(05\)70307-5](https://doi.org/10.1016/S0380-1330(05)70307-5), 2005.  
580
- 581 Cooperative Institute for Great Lakes Research, University of Michigan; NOAA Great Lakes  
582 Environmental Research Laboratory: Physical, chemical, and biological water quality monitoring  
583 data to support detection of Harmful Algal Blooms (HABs) in western Lake Erie, collected by the  
584 Great Lakes Environmental Research Laboratory and the Cooperative Institute for Great Lakes  
585 Research since 2012, NOAA National Centers for Environmental Information [data set],  
586 <https://doi.org/10.25921/11da-3x54>, 2019.
- 587 Cory, R. M., Davis, T. W., Dick, G. J., Johengen, T., Deneff, V. J., Berry, M. A., Page, S. E.,  
588 Watson, S. B., Yuhas, K., and Kling, G. W.: Seasonal Dynamics in Dissolved Organic Matter,  
589 Hydrogen Peroxide, and Cyanobacterial Blooms in Lake Erie, *Front. Mar. Sci.*, 3, 2016.
- 590 Cousino, L. K., Becker, R. H., and Zmijewski, K. A.: Modeling the effects of climate change on  
591 water, sediment, and nutrient yields from the Maumee River watershed, *J. Hydrol. Reg. Stud.*, 4,  
592 762–775, <https://doi.org/10.1016/j.ejrh.2015.06.017>, 2015.
- 593 Den Uyl, P. A., Harrison, S. B., Godwin, C. M., Rowe, M. D., Strickler, J. R., and Vanderploeg,  
594 H. A.: Comparative analysis of *Microcystis* buoyancy in western Lake Erie and Saginaw Bay of  
595 Lake Huron, *Harmful Algae*, 108, 102102, <https://doi.org/10.1016/j.hal.2021.102102>, 2021.
- 596 Den Uyl, P. A., Thompson, L. R., Errera, R. M., Birch, J. M., Preston, C. M., Ussler, W. I.,  
597 Yancey, C. E., Chaganti, S. R., Ruberg, S. A., Doucette, G. J., Dick, G. J., Scholin, C. A., and  
598 Goodwin, K. D.: Lake Erie field trials to advance autonomous monitoring of cyanobacterial  
599 harmful algal blooms, *Front. Mar. Sci.*, 9, <https://doi.org/10.3389/fmars.2022.1021952>, 2022.
- 600 Dolan, D. M. and Chapra, S. C.: Great Lakes total phosphorus revisited: 1. Loading analysis  
601 and update (1994–2008), *J. Gt. Lakes Res.*, 38, 730–740,  
602 <https://doi.org/10.1016/j.jglr.2012.10.001>, 2012.



- 603 Environment and Climate Change Canada and the U.S. Environmental Protection Agency.  
604 2022. State of the Great Lakes 2022 Technical Report. Cat No. En161-3/1E-PDF. EPA 905-  
605 R22-004. Available at binational.net, 2022.
- 606 Fang, S., Del Giudice, D., Scavia, D., Binding, C. E., Bridgeman, T. B., Chaffin, J. D., Evans, M.  
607 A., Guinness, J., Johengen, T. H., and Obenour, D. R.: A space-time geostatistical model for  
608 probabilistic estimation of harmful algal bloom biomass and areal extent, *Sci. Total Environ.*,  
609 695, 133776, <https://doi.org/10.1016/j.scitotenv.2019.133776>, 2019.
- 610 Goeyens, L., Kindermans, N., Abu Yusuf, M., and Elskens, M.: A Room Temperature Procedure  
611 for the Manual Determination of Urea in Seawater, *Estuar. Coast. Shelf Sci.*, 47, 415–418,  
612 <https://doi.org/10.1006/ecss.1998.0357>, 1998.
- 613 Hartig, J. H., Zarull, M. A., Ciborowski, J. J. H., Gannon, J. E., Wilke, E., Norwood, G., and  
614 Vincent, A. N.: Long-term ecosystem monitoring and assessment of the Detroit River and  
615 Western Lake Erie, *Environ. Monit. Assess.*, 158, 87–104, <https://doi.org/10.1007/s10661-008-0567-0>, 2009.
- 617 GLWQA: Great Lakes Water Quality Agreement; Protocol Amending the Agreement Between  
618 Canada and the United States of America on Great Lakes Water Quality, 1978, as Amended on  
619 October 16, 1983 and on November 18, 1987, <https://binational.net/2012/09/05/2012-glwqa-aqegl/> (last access: November 2022), 2012.  
620  
621
- 622 Hartig, J. H., Francoeur, S. N., Ciborowski, J. J. H., Gannon, J. E., Sanders, C. E., Galvao-  
623 Ferreira, P., Knauss, C. R., Gell, G., and Berk, K.: An ecosystem health assessment of the  
624 Detroit River and western Lake Erie, *J. Gt. Lakes Res.*, 47, 1241–1256,  
625 <https://doi.org/10.1016/j.jglr.2021.05.008>, 2021.
- 626 Hedges, J. I. and Stern, J. H.: Carbon and nitrogen determinations of carbonate-containing  
627 solids<sup>1</sup>, *Limnol. Oceanogr.*, 29, 657–663, <https://doi.org/10.4319/lo.1984.29.3.0657>, 1984.
- 628 Hellweger, F. L., Martin, R. M., Eigemann, F., Smith, D. J., Dick, G. J., and Wilhelm, S. W.:  
629 Models predict planned phosphorus load reduction will make Lake Erie more toxic, *Science*,  
630 376, 1001–1005, <https://doi.org/10.1126/science.abm6791>, 2022.
- 631 Hoffman, D. K., McCarthy, M. J., Boedecker, A. R., Myers, J. A., and Newell, S. E.: The role of  
632 internal nitrogen loading in supporting non-N-fixing harmful cyanobacterial blooms in the water  
633 column of a large eutrophic lake, *Limnol. Oceanogr.*, n/a, <https://doi.org/10.1002/lno.12185>,  
634 2022.
- 635 Horváth, H., Kovács, A. W., Riddick, C., and Présing, M.: Extraction methods for phycocyanin  
636 determination in freshwater filamentous cyanobacteria and their application in a shallow lake,  
637 *Eur. J. Phycol.*, 48, 278–286, <https://doi.org/10.1080/09670262.2013.821525>, 2013.
- 638 Huisman, J., Codd, G. A., Paerl, H. W., Ibelings, B. W., Verspagen, J. M. H., and Visser, P. M.:  
639 Cyanobacterial blooms | *Nature Reviews Microbiology*, *Nat. Rev. Microbiol.*, 16, 471–483,  
640 <https://doi.org/10.1038/s41579-018-0040-1>, 2018.
- 641 Joosse, P. J. and Baker, D. B.: Context for re-evaluating agricultural source phosphorus  
642 loadings to the Great Lakes, *Can. J. Soil Sci.*, 91, 317–327, <https://doi.org/10.4141/cjss10005>,  
643 2011.



- 644 Kane, D. D., Ludsin, S. A., Briland, R. D., Culver, D. A., and Munawar, M.: Ten+years gone:  
645 Continued degradation of offshore planktonic communities in U.S. waters of Lake Erie's western  
646 and central basins (2003–2013), *J. Gt. Lakes Res.*, 41, 930–933,  
647 <https://doi.org/10.1016/j.jglr.2015.06.002>, 2015.
- 648 Kast, J. B., Apostel, A. M., Kalcic, M. M., Muenich, R. L., Dagnew, A., Long, C. M., Evenson, G.,  
649 and Martin, J. F.: Source contribution to phosphorus loads from the Maumee River watershed to  
650 Lake Erie, *J. Environ. Manage.*, 279, 111803, <https://doi.org/10.1016/j.jenvman.2020.111803>,  
651 2021.
- 652 Kharbush, J. J., Smith, D. J., Powers, M., Vanderploeg, H. A., Fanslow, D., Robinson, R. S.,  
653 Dick, G. J., and Pearson, A.: Chlorophyll nitrogen isotope values track shifts between  
654 cyanobacteria and eukaryotic algae in a natural phytoplankton community in Lake Erie, *Org.*  
655 *Geochem.*, 128, 71–77, <https://doi.org/10.1016/j.orggeochem.2018.12.006>, 2019.
- 656 Kharbush, J. J., Robinson, R. S., and Carter, S. J.: Patterns in sources and forms of nitrogen in  
657 a large eutrophic lake during a cyanobacterial harmful algal bloom, *Limnol. Oceanogr.*, n/a,  
658 <https://doi.org/10.1002/lno.12311>, 2023.
- 659 King, W. M., Curless, S. E., and Hood, J. M.: River phosphorus cycling during high flow may  
660 constrain Lake Erie cyanobacteria blooms, *Water Res.*, 222, 118845,  
661 <https://doi.org/10.1016/j.watres.2022.118845>, 2022.
- 662 Liu, Q., Rowe, M. D., Anderson, E. J., Stow, C. A., Stumpf, R. P., and Johengen, T. H.:  
663 Probabilistic forecast of microcystin toxin using satellite remote sensing, in situ observations and  
664 numerical modeling, *Environ. Model. Softw.*, 128, 104705,  
665 <https://doi.org/10.1016/j.envsoft.2020.104705>, 2020.
- 666 Lunetta, R. S., Schaeffer, B. A., Stumpf, R. P., Keith, D., Jacobs, S. A., and Murphy, M. S.:  
667 Evaluation of cyanobacteria cell count detection derived from MERIS imagery across the  
668 eastern USA, *Remote Sens. Environ.*, 157, 24–34, <https://doi.org/10.1016/j.rse.2014.06.008>,  
669 2015.
- 670 Maguire, T. J., Stow, C. A., and Godwin, C. M.: Spatially referenced Bayesian state-space  
671 model of total phosphorus in western Lake Erie, *Hydrol. Earth Syst. Sci.*, 26, 1993–2017,  
672 <https://doi.org/10.5194/hess-26-1993-2022>, 2022.
- 673 Makarewicz, J. C. and Bertram, P.: Evidence for the Restoration of the Lake Erie Ecosystem:  
674 Water quality, oxygen levels, and pelagic function appear to be improving, *BioScience*, 41, 216–  
675 223, <https://doi.org/10.2307/1311411>, 1991.
- 676 Marino, J. A., Denef, V. J., Dick, G. J., Duhaime, M. B., and James, T. Y.: Fungal community  
677 dynamics associated with harmful cyanobacterial blooms in two Great Lakes, *J. Gt. Lakes Res.*,  
678 48, 1021–1031, <https://doi.org/10.1016/j.jglr.2022.05.007>, 2022.
- 679 Matisoff, G., Kaltenberg, E. M., Steely, R. L., Hummel, S. K., Seo, J., Gibbons, K. J.,  
680 Bridgeman, T. B., Seo, Y., Behbahani, M., James, W. F., Johnson, L. T., Doan, P., Dittrich, M.,  
681 Evans, M. A., and Chaffin, J. D.: Internal loading of phosphorus in western Lake Erie, *J. Gt.*  
682 *Lakes Res.*, 42, 775–788, <https://doi.org/10.1016/j.jglr.2016.04.004>, 2016.



- 683 Michalak, A. M., Anderson, E. J., Beletsky, D., Boland, S., Bosch, N. S., Bridgeman, T. B.,  
684 Chaffin, J. D., Cho, K., Confesor, R., Daloğlu, I., DePinto, J. V., Evans, M. A., Fahnenstiel, G. L.,  
685 He, L., Ho, J. C., Jenkins, L., Johengen, T. H., Kuo, K. C., LaPorte, E., Liu, X., McWilliams, M.  
686 R., Moore, M. R., Posselt, D. J., Richards, R. P., Scavia, D., Steiner, A. L., Verhamme, E.,  
687 Wright, D. M., and Zagorski, M. A.: Record-setting algal bloom in Lake Erie caused by  
688 agricultural and meteorological trends consistent with expected future conditions, *Proc. Natl.*  
689 *Acad. Sci.*, 110, 6448–6452, <https://doi.org/10.1073/pnas.1216006110>, 2013.
- 690 Mitchell, B.G., Kahru, M., Wieland, J., and Stramska, M.: Determination of spectral absorption  
691 coefficients of particles, dissolved material and phytoplankton for discrete water samples, In:  
692 Mueller, J.L., G.S. Fargion, and C.R. McClain [Eds.] *Ocean Optics Protocols for Satellite Ocean*  
693 *Color Sensor Validation, Revision 4, Volume IV: Inherent Optical Properties: Instruments,*  
694 *Characterizations, Field Measurements and Data Analysis Protocols. NASA/TM- 2003-211621,*  
695 *NASA Goddard Space Flight Center, Greenbelt, MD, Chapter 4, pp 39-64, 2003.*
- 696 Mohamed, M. N., Wellen, C., Parsons, C. T., Taylor, W. D., Arhonditsis, G., Chomicki, K. M.,  
697 Boyd, D., Weidman, P., Mundle, S. O. C., Cappellen, P. V., Sharpley, A. N., and Haffner, D. G.:  
698 Understanding and managing the re-eutrophication of Lake Erie: Knowledge gaps and research  
699 priorities, *Freshw. Sci.*, 38, 675–691, <https://doi.org/10.1086/705915>, 2019.
- 700 Mulvenna, P. F. and Savidge, G.: A modified manual method for the determination of urea in  
701 seawater using diacetylmonoxime reagent, *Estuar. Coast. Shelf Sci.*, 34, 429–438,  
702 [https://doi.org/10.1016/S0272-7714\(05\)80115-5](https://doi.org/10.1016/S0272-7714(05)80115-5), 1992.
- 703 Myers, D.N., Thomas, M.A., Frey, J.W., Rheaume, S.J., and Button, D.T.: Water Quality in the  
704 Lake Erie-Lake Saint Clair Drainages Michigan, Ohio, Indiana, New York, and Pennsylvania,  
705 1996–98: U.S. Geological Survey Circular 1203, 35 p., <https://pubs.water.usgs.gov/circ1203/>,  
706 2000.  
707
- 708 Newell, S. E., Davis, T. W., Johengen, T. H., Gossiaux, D., Burtner, A., Palladino, D., and  
709 McCarthy, M. J.: Reduced forms of nitrogen are a driver of non-nitrogen-fixing harmful  
710 cyanobacterial blooms and toxicity in Lake Erie, *Harmful Algae*, 81, 86–93,  
711 <https://doi.org/10.1016/j.hal.2018.11.003>, 2019.
- 712 Pirasteh, S., Mollae, S., Fathollahi, S. N., and Li, J.: Estimation of Phytoplankton Chlorophyll-a  
713 Concentrations in the Western Basin of Lake Erie Using Sentinel-2 and Sentinel-3 Data, *Can. J.*  
714 *Remote Sens.*, 46, 585–602, <https://doi.org/10.1080/07038992.2020.1823825>, 2020.
- 715 Prater, C., Frost, P. C., Howell, E. T., Watson, S. B., Zastepa, A., King, S. S. E., Vogt, R. J., and  
716 Xenopoulos, M. A.: Variation in particulate C : N : P stoichiometry across the Lake Erie  
717 watershed from tributaries to its outflow, *Limnol. Oceanogr.*, 62, S194–S206,  
718 <https://doi.org/10.1002/lno.10628>, 2017.
- 719 Qian, S. S., Stow, C. A., Rowland, F. E., Liu, Q., Rowe, M. D., Anderson, E. J., Stumpf, R. P.,  
720 and Johengen, T. H.: Chlorophyll a as an indicator of microcystin: Short-term forecasting and  
721 risk assessment in Lake Erie, *Ecol. Indic.*, 130, 108055,  
722 <https://doi.org/10.1016/j.ecolind.2021.108055>, 2021.
- 723 Reavie, E. D., Cai, M., Twiss, M. R., Carrick, H. J., Davis, T. W., Johengen, T. H., Gossiaux, D.,  
724 Smith, D. E., Palladino, D., Burtner, A., and Sgro, G. V.: Winter–spring diatom production in



- 725 Lake Erie is an important driver of summer hypoxia, *J. Gt. Lakes Res.*, 42, 608–618,  
726 <https://doi.org/10.1016/j.jglr.2016.02.013>, 2016.
- 727 Rowe, M. D., Anderson, E. J., Wynne, T. T., Stumpf, R. P., Fanslow, D. L., Kijanka, K.,  
728 Vanderploeg, H. A., Strickler, J. R., and Davis, T. W.: Vertical distribution of buoyant *Microcystis*  
729 blooms in a Lagrangian particle tracking model for short-term forecasts in Lake Erie, *J.*  
730 *Geophys. Res. Oceans*, 121, 5296–5314, <https://doi.org/10.1002/2016JC011720>, 2016.
- 731 Rowland, F. E., Stow, C. A., Johengen, T. H., Burtner, A. M., Palladino, D., Gossiaux, D. C.,  
732 Davis, T. W., Johnson, L. T., and Ruberg, S.: Recent Patterns in Lake Erie Phosphorus and  
733 Chlorophyll *a* Concentrations in Response to Changing Loads, *Environ. Sci. Technol.*, 54, 835–  
734 841, <https://doi.org/10.1021/acs.est.9b05326>, 2020.
- 735 Sayers, M., Fahnenstiel, G. L., Shuchman, R. A., and Whitley, M.: Cyanobacteria blooms in  
736 three eutrophic basins of the Great Lakes: a comparative analysis using satellite remote  
737 sensing, *Int. J. Remote Sens.*, 37, 4148–4171, <https://doi.org/10.1080/01431161.2016.1207265>,  
738 2016.
- 739 Sayers, M. J., Bosse, K. R., Shuchman, R. A., Ruberg, S. A., Fahnenstiel, G. L., Leshkevich, G.  
740 A., Stuart, D. G., Johengen, T. H., Burtner, A. M., and Palladino, D.: Spatial and temporal  
741 variability of inherent and apparent optical properties in western Lake Erie: Implications for  
742 water quality remote sensing, *J. Gt. Lakes Res.*, 45, 490–507,  
743 <https://doi.org/10.1016/j.jglr.2019.03.011>, 2019.
- 744 Smith, D. J., Tan, J. Y., Powers, M. A., Lin, X. N., Davis, T. W., and Dick, G. J.: Individual  
745 *Microcystis* colonies harbour distinct bacterial communities that differ by *Microcystis* oligotype  
746 and with time, *Environ. Microbiol.*, 23, 3020–3036, <https://doi.org/10.1111/1462-2920.15514>,  
747 2021.
- 748 Smith, D. J., Berry, M. A., Cory, R. M., Johengen, T. H., Kling, G. W., Davis, T. W., and Dick, G.  
749 J.: Heterotrophic Bacteria Dominate Catalase Expression during *Microcystis* Blooms, *Appl.*  
750 *Environ. Microbiol.*, 88, e02544-21, <https://doi.org/10.1128/aem.02544-21>, 2022.
- 751 Smith, R. B., Bass, B., Sawyer, D., Depew, D., and Watson, S. B.: Estimating the economic  
752 costs of algal blooms in the Canadian Lake Erie Basin, *Harmful Algae*, 87, 101624,  
753 <https://doi.org/10.1016/j.hal.2019.101624>, 2019.
- 754 Speziale, B. J., Schreiner, S. P., Giammatteo, P. A., and Schindler, J. E.: Comparison of N,N-  
755 Dimethylformamide, Dimethyl Sulfoxide, and Acetone for Extraction of Phytoplankton  
756 Chlorophyll, *Can. J. Fish. Aquat. Sci.*, 41, 1519–1522, <https://doi.org/10.1139/f84-187>, 1984.
- 757 Standard Methods Committee of the American Public Health Association, American Water  
758 Works Association, and Water Environment Federation: Standard Methods For the Examination  
759 of Water and Wastewater, 23<sup>rd</sup> edition, Sections 2540 Solids, 4500-P Phosphorus, 4500-nh3-  
760 nitrogen (ammonia), 4500-no3-nitrogen (nitrate), 5310 Total Organic Carbon, edited by: Lipps  
761 WC, Baxter TE, Braun-Howland E, APHA Press, Washington, DC, ISBN 1625762402, 2017.
- 762 Steffen, M. M., Belisle, B. S., Watson, S. B., Boyer, G. L., and Wilhelm, S. W.: Status, causes  
763 and controls of cyanobacterial blooms in Lake Erie, *J. Gt. Lakes Res.*, 40, 215–225,  
764 <https://doi.org/10.1016/j.jglr.2013.12.012>, 2014.



- 765 Steffen, M. M., Davis, T. W., McKay, R. M. L., Bullerjahn, G. S., Krausfeldt, L. E., Stough, J. M.  
766 A., Neitzey, M. L., Gilbert, N. E., Boyer, G. L., Johengen, T. H., Gossiaux, D. C., Burtner, A. M.,  
767 Palladino, D., Rowe, M. D., Dick, G. J., Meyer, K. A., Levy, S., Boone, B. E., Stumpf, R. P.,  
768 Wynne, T. T., Zimba, P. V., Gutierrez, D., and Wilhelm, S. W.: Ecophysiological Examination of  
769 the Lake Erie Microcystis Bloom in 2014: Linkages between Biology and the Water Supply  
770 Shutdown of Toledo, OH, *Environ. Sci. Technol.*, 51, 6745–6755,  
771 <https://doi.org/10.1021/acs.est.7b00856>, 2017.
- 772 Sterner, R. W., Keeler, B., Polasky, S., Poudel, R., Rhude, K., and Rogers, M.: Ecosystem  
773 services of Earth's largest freshwater lakes, *Ecosyst. Serv.*, 41, 101046,  
774 <https://doi.org/10.1016/j.ecoser.2019.101046>, 2020.
- 775 Stow, C. A., Cha, Y., Johnson, L. T., Confesor, R., and Richards, R. P.: Long-Term and  
776 Seasonal Trend Decomposition of Maumee River Nutrient Inputs to Western Lake Erie, *Environ.*  
777 *Sci. Technol.*, 49, 3392–3400, <https://doi.org/10.1021/es5062648>, 2015.
- 778 US EPA - United States Environmental Protection Agency: Method 180.1: Determination of  
779 Turbidity by Nephelometry, Revision 2.0, Edited by: O'Dell, J.W., 1993.
- 780 US EPA - United States Environmental Protection Agency: Drinking Water Health Advisory for  
781 the Cyanobacterial Microcystin Toxins, EPA Document Number 820R15100, 2015.  
782
- 783 Van Meter, K. J., McLeod, M. M., Liu, J., Tenkouano, G. T., Hall, R. I., Van Cappellen, P., and  
784 Basu, N. B.: Beyond the Mass Balance: Watershed Phosphorus Legacies and the Evolution of  
785 the Current Water Quality Policy Challenge, *Water Resour. Res.*, 57, e2020WR029316,  
786 <https://doi.org/10.1029/2020WR029316>, 2021.
- 787 Vander Woude, A., Ruberg, S., Johengen, T., Miller, R., and Stuart, D.: Spatial and temporal  
788 scales of variability of cyanobacteria harmful algal blooms from NOAA GLERL airborne  
789 hyperspectral imagery, *J. Gt. Lakes Res.*, 45, 536–546,  
790 <https://doi.org/10.1016/j.jglr.2019.02.006>, 2019.
- 791 Vanderploeg, H. A., Liebig, J. R., Carmichael, W. W., Agy, M. A., Johengen, T. H., Fahnenstiel,  
792 G. L., and Nalepa, T. F.: Zebra mussel (*Dreissena polymorpha*) selective filtration promoted  
793 toxic *Microcystis* blooms in Saginaw Bay (Lake Huron) and Lake Erie, *Can. J. Fish. Aquat. Sci.*,  
794 58, 1208–1221, <https://doi.org/10.1139/f01-066>, 2001.
- 795 Wang, Q. and Boegman, L.: Multi-Year Simulation of Western Lake Erie Hydrodynamics and  
796 Biogeochemistry to Evaluate Nutrient Management Scenarios, *Sustainability*, 13, 7516,  
797 <https://doi.org/10.3390/su13147516>, 2021.
- 798 Watson, S. B., Miller, C., Arhonditsis, G., Boyer, G. L., Carmichael, W., Charlton, M. N.,  
799 Confesor, R., Depew, D. C., Höök, T. O., Ludsin, S. A., Matisoff, G., McElmurry, S. P., Murray,  
800 M. W., Peter Richards, R., Rao, Y. R., Steffen, M. M., and Wilhelm, S. W.: The re-eutrophication  
801 of Lake Erie: Harmful algal blooms and hypoxia, *Harmful Algae*, 56, 44–66,  
802 <https://doi.org/10.1016/j.hal.2016.04.010>, 2016.
- 803 Weiskerger, C. J., Rowe, M. D., Stow, C. A., Stuart, D., and Johengen, T.: Application of the  
804 Beer–Lambert Model to Attenuation of Photosynthetically Active Radiation in a Shallow,  
805 Eutrophic Lake, *Water Resour. Res.*, 54, 8952–8962, <https://doi.org/10.1029/2018WR023024>,  
806 2018.



- 807 Wetzell, R.G., and Likens G.E.: Limnological Analyses, 3<sup>rd</sup> edition, Springer New York, NY,  
808 <https://doi.org/10.1007/978-1-4757-3250-4>, 2000.
- 809 WHO - World Health Organization: Cyanobacterial toxins: microcystins. Background document  
810 for development of WHO Guidelines for drinking-water quality and Guidelines for safe  
811 recreational water environments, WHO/HEP/ECH/WSH/2020.6, 2020.  
812
- 813 Wilson, A. E., Gossiaux, D. C., Höök, T. O., Berry, J. P., Landrum, P. F., Dyble, J., and  
814 Guildford, S. J.: Evaluation of the human health threat associated with the hepatotoxin  
815 microcystin in the muscle and liver tissues of yellow perch (*Perca flavescens*), *Can. J. Fish.*  
816 *Aquat. Sci.*, 65, 1487–1497, <https://doi.org/10.1139/F08-067>, 2008.
- 817 Wynne, T. T., Stumpf, R. P., Tomlinson, M. C., Fahnenstiel, G. L., Dyble, J., Schwab, D. J., and  
818 Joshi, S. J.: Evolution of a cyanobacterial bloom forecast system in western Lake Erie:  
819 Development and initial evaluation, *J. Gt. Lakes Res.*, 39, 90–99,  
820 <https://doi.org/10.1016/j.jglr.2012.10.003>, 2013.
- 821 Xu, J., Liu, H., Lin, J., Lyu, H., Dong, X., Li, Y., Guo, H., and Wang, H.: Long-term monitoring  
822 particulate composition change in the Great Lakes using MODIS data, *Water Res.*, 222,  
823 118932, <https://doi.org/10.1016/j.watres.2022.118932>, 2022.
- 824 Yancey, C.E., Mathiesen, O., and Dick, G.J.: Transcriptionally active nitrogen fixation and  
825 biosynthesis of diverse secondary metabolites by *Dolichospermum* and *Aphanizominom*-like  
826 *Cyanobacteria* in western Lake Erie *Microcystis* blooms, *bioRxiv* [preprint],  
827 <https://doi.org/10.1101/2022.09.30.510322> 01 October 2022a.
- 828 Yancey, C. E., Smith, D. J., Den Uyl, P. A., Mohamed, O. G., Yu, F., Ruberg, S. A., Chaffin, J.  
829 D., Goodwin, K. D., Tripathi, A., Sherman, D. H., and Dick, G. J.: Metagenomic and  
830 Metatranscriptomic Insights into Population Diversity of *Microcystis* Blooms: Spatial and  
831 Temporal Dynamics of *mcy* Genotypes, Including a Partial Operon That Can Be Abundant and  
832 Expressed, *Appl. Environ. Microbiol.*, 88, e02464-21, <https://doi.org/10.1128/aem.02464-21>,  
833 2022b.